

## Perspectives for antideuteron search in Cosmic Rays with a helium pressurized calorimeter

F. ROSSI<sup>(1)(2)</sup>, G. GIOVANAZZI<sup>(2)</sup>, F. NOZZOLI<sup>(1)(2)</sup>, L. RICCI<sup>(2)</sup>, P. SPINNATO<sup>(1)</sup>, E. VERROI<sup>(1)</sup>, and P. ZUCCON<sup>(1)(2)</sup>

<sup>(1)</sup> *INFN-TIFPA, Trento, Italy*

<sup>(2)</sup> *Dipartimento di Fisica, Università di Trento - Trento, Italy*

**Summary.** — The search for antideuterons in Cosmic Rays (CRs) addresses fundamental questions such as the nature of Dark Matter or the presence of primordial antimatter. The Pressurized Helium Scintillating Calorimeter for AntiMatter Identification (PHeSCAMI) project aims to identify low-energy antideuterons in CRs, through delayed annihilations within a helium target. The performance of a possible large-acceptance detector based on the detection technique of the PHeSCAMI project is presented. In particular, we developed a possible trigger logic and estimated the expected background rate for the proposed design, using a Monte Carlo simulation based on the Geant4 toolkit.

### 1. – Introduction

The presence of low energy antideuterons,  $\bar{d}$ , in Cosmic Rays (CRs) is considered a golden channel for identifying Dark Matter (DM) annihilation or the presence of primordial antimatter in our galaxy. As shown by the PHENIX [1] and ALICE [2] collaboration, low-energy antideuterons are unlikely to be produced as secondary particles in CRs propagation processes. Considering current space experiments the investigation of complex antinuclei in CRs has therefore a negligible astrophysical background.

The PHeSCAMI detector aims to identify  $Z=-1$  antinuclei in Cosmic Rays. The incoming antiparticles can stop inside an helium target, creating an exotic helium atom in a meta-stable state [3]. A fraction of these meta-stable states atoms has a long lifetime  $\sim \mu s$ , for  $\bar{p}$  such fraction is  $\sim 3.3\%$ , giving rise to a delayed annihilation.

The performances of a possible large-acceptance detector based on the PHeSCAMI project are investigated in the following using a Monte Carlo simulation based on the Geant4 toolkit [4, 5, 6].

## 2. – A possible PHeSCAMI detector

Figure 1 shows a graphical representation of the PHeSCAMI detector and an example of  $\bar{d}$  undergoing a delayed annihilation. The simulated PHeSCAMI design comprises two sub-detectors: a Time of Flight (TOF) and a segmented helium calorimeter (HeCal). Two layers of segmented plastic scintillators build up the TOF system. Each layer has a cubic shape, where 64 slabs of 0.4 cm thick compose each face. The sides of the external TOF layer are 3 m long and the distance between the external and the internal TOF layers is 20 cm. The HeCal comprises 75 helium tanks (50 L each) operating at a nominal pressure of 310 bar. Helium is a fast ( $\tau \sim 5\text{ ns}$ ) scintillator allowing the measurement of the deposited energy with a time resolution typically better than 300 ps [3]. The mass budget and geometry of the helium tanks reproduce the state-of-art values for space-qualified tanks for pressurized helium [7].

Particle identification is possible by combining the velocity measurement  $\beta$ , along with the measurements of energy losses ( $\frac{dE}{dx}$ ) with the TOF and the calorimetric measurement of the residual energy with the HeCal. The TOF energy resolution implemented in the detector simulation is  $\frac{\sigma_E}{E} = 5\%$ , whilst the velocity resolution is  $\frac{\sigma_\beta}{\beta} = 5\%$ . The energy resolution goal for the HeCal is  $\frac{\sigma_E}{E} = 10\%$ .

In the simulation, particles are generated isotropically from a plane of  $15.2 \times 15.2 \text{ m}^2$  placed on top of the detector. The energy distributions of the low energy  $\bar{d}$  and  $\bar{p}$  were generated assuming a power law of  $(E_K/N)^{-1}$ , where  $E_K/N$  is the kinetic energy per nucleon. For the evaluation of the detector background, the measured fluxes archived in the Cosmic Ray Database (CRDB) [8] were considered for ordinary matter particles and nuclei as protons, electrons,  $^4\text{He}$  and  $^{12}\text{C}$ .

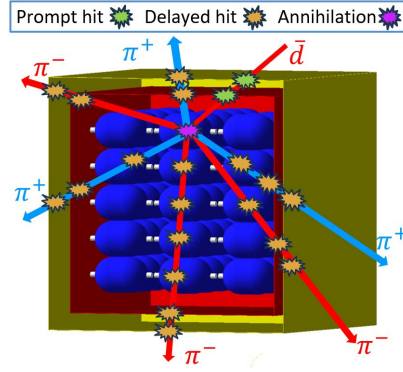


Fig. 1. – Pictorial representation of  $\bar{d}$  annihilation inside the PHeSCAMI detector. Two layers of segmented plastic scintillators (in red and yellow) build up the TOF. The HeCal is made of helium tanks presented in blue. The detector's overall volume is  $27 \text{ m}^3$ . Prompt and delayed hits are referring to energy depositions occurring within or after 50 ns (see sec. 3).

## 3. – Trigger logic

The trigger logic of the PHeSCAMI detector is optimized to reject the large fraction of ordinary Minimum Ionizing Particles (MIPs) in the CRs and identify delayed annihilations produced by slow antinuclei stopping in the helium scintillator. A two-step trigger logic has been developed for this task. The first trigger level, named *prompt trigger*,

focuses on MIPs rejection and selects events where the particle stops inside the detector. If the *prompt trigger* condition is satisfied, a gate of  $3.95\mu\text{s}$  is opened 50 ns after the *prompt trigger* waiting for a *delayed trigger*, that is looking for the evidence of a delayed annihilation. If also the *delayed trigger* condition is satisfied the event is acquired and stored on disk.

The *prompt trigger* exploits the different deposited energy between a  $Z=1$  MIP and a particle stopping inside the detector. Stopping particles are slower and suffer larger energy losses as compared to MIPs. Another difference arises from the number of hits inside the TOF, i.e. the number of scintillator slabs with an energy deposition above the threshold, since a MIP will cross the whole detector providing four TOF hits. The overall MIP rejection power can be improved by combining this information, i.e. requiring for each TOF layer a hit with an energy deposit larger than  $2\text{MIP}_{\text{TOF}}$  corresponding to 1.6 MeV. Moreover, only one additional TOF hit with an energy deposit larger than  $1\text{MIP}_{\text{TOF}}$ , i.e. 0.8 MeV is allowed. Regarding the HeCal it is required the presence of one HeCal module with deposited energy larger than  $1.3\text{MIP}_{\text{HeCal}}$ , corresponding to 10 MeV, tagging a stopping particle.

The delayed annihilations of  $\bar{d}$  and  $\bar{p}$  produce secondary pions. The average number of pions is roughly proportional to the number of annihilating nucleons. In particular, 3 charged pions are expected for  $\bar{p}$ , whilst 6 charged pions for  $\bar{d}$ , on average. For this reason, the total energy deposits on both the TOF layers and inside the HeCal are expected to be twice for  $\bar{d}$  compared to  $\bar{p}$ . The annihilation topology should produce measurable signals on at least 4 different scintillator slabs in the TOF. On the other hand, to minimize the possible background contribution due to the accidental pile-up of a nucleus fragmenting in the HeCal, an energy deposition lower than  $2\text{MIP}_{\text{TOF}}$  is required.

Summarizing, both triggers discriminate against two different energy thresholds, here normalized to a MIP energy deposition for simplicity. In particular, for this design of the PHeSCAMI detector, the most probable value for a MIP energy deposit is 0.8 MeV for the scintillators composing the TOF and 7.5 MeV for the helium tanks of the HeCal. Thus, the *prompt trigger* thresholds are set to  $2\text{MIP}_{\text{TOF}} = 1.6\text{ MeV}$  and  $1.3\text{MIP}_{\text{HeCal}} = 10\text{ MeV}$ , whilst the *delayed trigger* has a different TOF energy threshold corresponding to  $1\text{MIP}_{\text{TOF}} = 0.8\text{ MeV}$  but the same HeCal threshold. Events not satisfying all the requirements of the two trigger selections are discarded or prescaled. The table I summarises the trigger conditions.

The loss of signal efficiency due to the trigger thresholds is negligible, indeed the expected energy losses for  $\bar{d}$  stopping inside the PHeSCAMI detector ranges from 1.6 MeV up to 15 MeV, for the maximum energy deposit on a single TOF slab, while the expected maximum signal in the HeCal goes from 10 MeV up to 70 MeV. The estimated energy releases after the delayed annihilation range from 0.8 MeV up to 40 MeV for a single TOF

Prompt Trigger	Delayed Trigger
Max $E_{\text{dep}}$ outer TOF $> 2\text{MIP}_{\text{TOF}}$	$2\text{MIP}_{\text{TOF}} > \text{Max } E_{\text{dep}}$ outer TOF $> 1\text{MIP}_{\text{TOF}}$
Max $E_{\text{dep}}$ inner TOF $> 2\text{MIP}_{\text{TOF}}$	$2\text{MIP}_{\text{TOF}} > \text{Max } E_{\text{dep}}$ inner TOF $> 1\text{MIP}_{\text{TOF}}$
Max $E_{\text{dep}}$ HeCal $> 1.3\text{MIP}_{\text{HeCal}}$	Max $E_{\text{dep}}$ HeCal $> 1.3\text{MIP}_{\text{HeCal}}$
TOF prompt hits $\leq 3$	TOF delayed hits $> 4$

TABLE I. –  $\text{MIP}_{\text{TOF}}$  corresponds to 0.8 MeV and  $\text{MIP}_{\text{HeCal}}$  to 7.5 MeV. The prompt TOF hits are the number of slabs with an  $E_{\text{dep}} > 1\text{MIP}_{\text{TOF}}$ , whilst the delayed TOF hits have an  $E_{\text{dep}}$  between  $\in (1\text{MIP}_{\text{TOF}}, 2\text{MIP}_{\text{TOF}})$ .

slab, and from 10 MeV to 100 MeV inside the HeCal.

#### 4. – Expected background rate and trigger acceptance

The expected trigger rate of this possible design for the PHeSCAMI detector is evaluated by considering the background provided by the most abundant particles and nuclei in CRs. In particular, protons,  ${}^4\text{He}$ ,  ${}^{12}\text{C}$  and electrons have been simulated. The rate in each bin of kinetic energy per nucleon is calculated using:

$$R[\text{s}^{-1}] = \int \phi[\text{GeV} \cdot \text{s} \cdot \text{m}^2 \cdot \text{sr}]^{-1} \cdot G[\text{m}^2 \cdot \text{sr}] dE$$

where  $\phi$  is the particle flux modelled according to existing measurements [8] and  $G$  is the trigger acceptance. Acceptances are obtained by independently applying the two triggers, accounting for pile-up effects within the delayed coincidence gate. Void histograms on the left plot of figure 2 show the expected rate in each kinetic energy bin for events providing a *prompt trigger*. Analogously, the filled histogram presents the expected rates for events providing a *delayed trigger*. The expected acquisition rate is the product of the *prompt trigger* rate (9 kHz) the *delayed trigger* rate (2.7 kHz) and the  $3.95 \mu\text{s}$  gate width. Considering the background due to ordinary CRs, the expected DAQ rate is  $\sim 100$  Hz, and DAQ dead time is below 5%.

The trigger acceptances for antiparticles (i.e.  $\bar{d}$  and  $\bar{p}$ ) are obtained by applying the trigger conditions presented in section 3. The results, in the right plot of figure 2, take into account the probability of creating a meta-stable state ( $\sim 3.3\%$ ) and of annihilating within the time window  $\in [50, 4000] \text{ ns}$ . The maximum trigger acceptance for  $\bar{d}$  is  $0.7 \text{ m}^2\text{sr}$  at  $E_K/N = 50 \text{ MeV}$  and falls steeply after  $E_K/N = 80 \text{ MeV}$ . The acceptance for  $\bar{p}$  has a maximum of  $0.23 \text{ m}^2\text{sr}$  at  $E_K/N = 70 \text{ MeV}$  and continues to decrease for kinetic energies higher than  $E_K/N = 110 \text{ MeV}$ . This configuration of the PHeSCAMI detector is sensible in the low kinetic energy range, between  $\in [40, 50] \text{ MeV}$  for  $\bar{d}$  and between  $\in [60, 80]$  for  $\bar{p}$ .

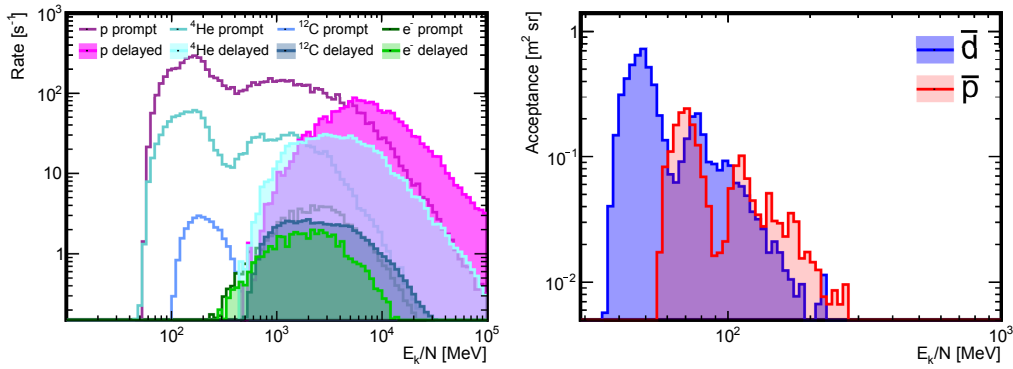


Fig. 2. – The left plot shows the trigger rates as a function of the kinetic energy per nucleon for  $p$ ,  ${}^4\text{He}$ ,  ${}^{12}\text{C}$  and  $e^-$ . Void histograms show the expected prompt trigger rates and filled histograms show the delayed trigger rates. The right plot shows the trigger acceptances for  $\bar{d}$  and  $\bar{p}$  as a function of the kinetic energy per nucleon.

### 5. – Antideuteron identification

After the acquisition of the events, an offline analysis is necessary to identify the possible  $\bar{d}$  signal from the other particle background. Here a preliminary investigation of the capability to disentangle  $\bar{d}$  from  $\bar{p}$  is shown.

The left plot in figure 3 shows the velocity reconstructed by the TOF against the energy promptly released within the HeCal. The right plot in figure 3 reports the specific energy loss measured by the external TOF layer against the energy promptly released within the HeCal. Energy losses are normalized to the most probable value expected for MIP, corresponding to 2 MeV/cm. Thanks to the different masses, for fixed energy deposition in HeCal, the  $\bar{d}$  velocity ( $\beta = \frac{v}{c}$ ) is smaller than the  $\bar{p}$  one and energy losses higher. This allows a good separation between the two populations.

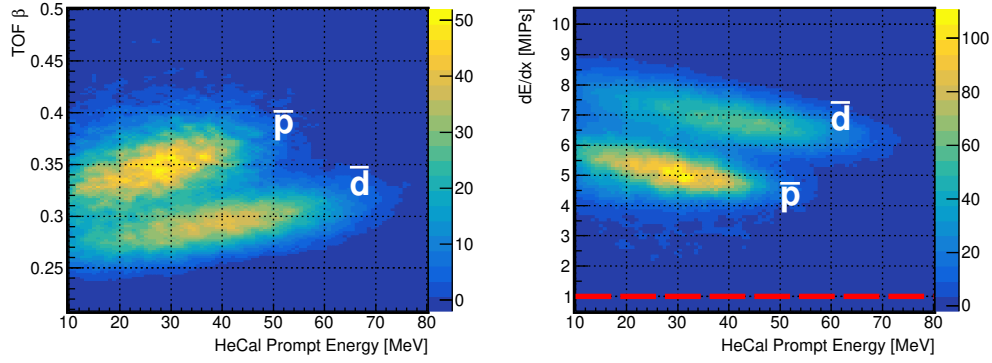


Fig. 3. – The left plot shows the velocity reconstructed with the TOF as a function of the energy promptly released within the HeCal. The right plot shows the specific energy loss measured by the external TOF layer, normalized to the MIP.

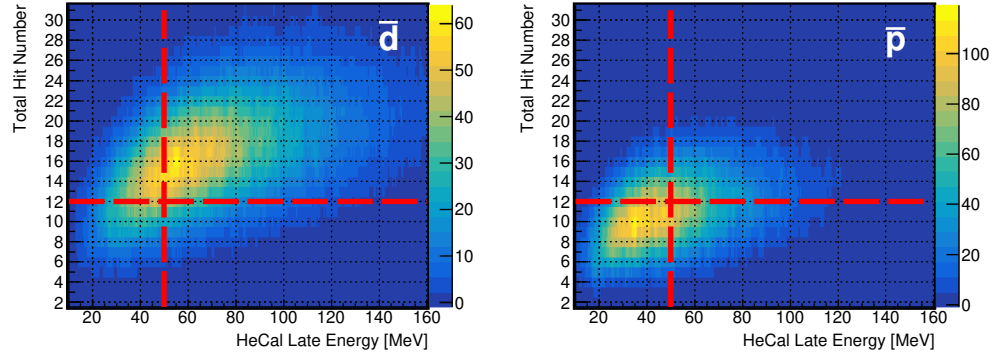


Fig. 4. – The two plots show the total number of hits (TOF+HeCal) as a function of the energy released by the delayed event inside the HeCal. The left panel presents the distribution for  $\bar{d}$ , whilst the right panel presents the  $\bar{p}$ . To guide the eye, the red dashed lines mark the separation between  $\bar{d}$  and  $\bar{p}$ .

The plots in figure 4 show the total number of scintillators slab and helium tanks with a signal over the MIP threshold, in the *delayed trigger*, as a function of the delayed

energy deposit in the HeCal. The left plot shows the distribution for  $\bar{d}$ , while the right plot reports the result for  $\bar{p}$ . Due to the higher multiplicity of charged particles,  $\bar{d}$  annihilations produce more hits than  $\bar{p}$ . This allows an additional identification tool for  $\bar{d}$  rejecting  $\bar{p}$ , the expected separation power will strongly improve with a tracking algorithm and multivariate techniques.

## 6. – Conclusions

The simulation of a large-acceptance detector based on the PHeSCAMI signature for antideuterons provides a geometrical acceptance maximum value of  $0.7 \text{ m}^2 \text{ sr}$  for  $\bar{d}$  and  $0.23 \text{ m}^2 \text{ sr}$  for  $\bar{p}$ . The highest sensitivity is reached in the ranges:  $E_K/N \in (40, 55) \text{ MeV}$  for  $\bar{d}$ , and  $E_K/N \in (60, 75) \text{ MeV}$  for  $\bar{p}$ . With the proposed design, the expected DAQ rate due to the background of ordinary CRs is  $\sim 100 \text{ Hz}$  with negligible dead time, thanks to the good rejection capabilities due to the peculiar detection signature. The identification of  $\bar{d}$  from the  $\bar{p}$  background is based on the differences in velocity, energy losses and annihilation topology.

\* \* \*

This work has been funded by the Italian Ministerial grant PRIN-2022 n.2022LLCPMH “PHeSCAMI-Pressurized Helium Scintillating Calorimeter for AntiMatter Identification”, CUP E53D23002100006. This publication was produced while F.R. attending the PhD program in Space Science and Technology at the University of Trento, Cycle XXXVIII, with the support of a scholarship financed by the Ministerial Decree no. 351 of 9th April 2022, based on the NRRP-funded by the European Union - NextGenerationEU - Mission 4 ”Education and Research”, Component 1 ”Enhancement of the offer of educational services: from nurseries to universities” - Investment 4.1 “Extension of the number of research doctorates and innovative doctorates for public administration and cultural heritage” - CUP E63C22001340001

## REFERENCES

- [1] S. S. Adler and et al. (PHENIX Collaboration). Deuteron and antideuteron production in Au + Au collisions at  $\sqrt{s_{NN}} = 200 \text{ GeV}$ . *Phys. Rev. Lett.*, 94:122302, Apr 2005.
- [2] S. Acharya and et al. (ALICE Collaboration). Measurement of anti-3He nuclei absorption in matter and impact on their propagation in the galaxy. *Nature Physics*, 19(1):61–71, December 2022.
- [3] Francesco Nozzoli, Irina Rashevskaya, Leonardo Ricci, Francesco Rossi, Piero Spinnato, Enrico Verroi, Paolo Zuccon, and Gregorio Giovanazzi. Antideuteron identification in space with helium calorimeter. *Instruments*, 8(1), 2024.
- [4] S. Agostinelli and et al. (GEANT4 collaboration). Geant4—a simulation toolkit. *Nuclear Instruments and Methods in Physics Research Section A: Accelerators, Spectrometers, Detectors and Associated Equipment*, 506(3):250–303, 2003.
- [5] J. Allison and et al. (GEANT4 collaboration). Geant4 developments and applications. *IEEE Transactions on Nuclear Science*, 53(1):270–278, 2006.
- [6] J. Allison and et al. (GEANT4 collaboration). Recent developments in geant4. *Nuclear Instruments and Methods in Physics Research Section A: Accelerators, Spectrometers, Detectors and Associated Equipment*, 835:186–225, 2016.
- [7] MT Areospace AG. *High Pressure Tank–Helium–COTS*.
- [8] David Maurin, Markus Ahlers, Hans Dembinski, Andreas Haungs, Pierre-Simon Mangeard, Frédéric Melot, Philipp Mertsch, Doris Wochele, and Jürgen Wochele. A cosmic-ray database update: Crdb v4.1. *The European Physical Journal C*, 83(10), October 2023.